Area V4 in *Cebus* Monkey: Extent and Visuotopic Organization

Maria Carmen Piñon, Ricardo Gattass and Aglai P.B. Sousa

Laboratório de Fisiologia da Cognição, Departamento de Neurobiologia, IBCCFᵒ, UFRJ, Rio de Janeiro, Brasil

We used electrophysiological mapping and myeloarchitectural criteria in order to define the location, extent and visual topography of the fourth visual area (V4) in anesthetized and paralyzed *Cebus* monkey. Based on these criteria, the borders of V4 with surrounding areas were defined both on the dorsal and ventral cortical surfaces. In addition, to better visualize the visuotopic organization and to evaluate its regularity, we constructed bidimensional maps and projected the recording sites onto them. Area V4 has an almost complete representation of the binocular visual field with the lower visual field represented dorsally (V4d) and the upper field ventrally (V4v). We found this representation to be more extensive than those previously described. The representation of the central portion of the visual field is largely expanded in comparison with that of the periphery. This emphasis in central vision could be related with the involvement of V4 in the ventral stream of visual information processing. Receptive field size increases with increasing eccentricity, while cortical magnification factor decreases. The cortical magnification factor measured along isopolar lines is, on average, 1.5–2.0 times greater than that measured along the isoeccentric lines, suggesting the existence of a small anisotropy in central and peripheral V4.

Introduction

Zeki (1971) first defined area V4 in *Macaca mullata* as an area receiving projections from the second and third visual areas (V2 and V3). This region, containing the representation of the central portion of the lower quadrant of the visual field, was subdivided into areas V4, located in the anterior bank of lunate sulcus, and V4A, in the prelunate gyrus. Later, Van Essen and Zeki (1978) studied part of the prelunate gyrus representing the central portion of the inferior quadrant and named this region the 'V4 complex'. According to these authors, 'V4 complex' does not contain a single, orderly representation of either the visual quadrant or the hemifield.

Maguire and Baizer (1984) studied the visual topography of the prelunate gyrus and surrounding cortex in awake behaving monkeys, and subdivided the 'V4 complex' into two areas: anterior lateral (AL) and posterior medial (PM), each containing the representation of 30° of the inferior visual quadrant. According to these authors the vertical meridian crosses the prelunate gyrus horizontally and defines the border between areas AL and PM. In addition, area AL includes the anterior part of the prelunate gyrus and the posterior portion of superior temporal sulcus, while area PM includes the rest of the prelunate gyrus and the anterior portion of lunate sulcus. These authors suggest that area AL could be part of the 'V4 complex', while area PM could be part of either the 'V4 complex' or of area V3A.

On the other hand, Gattass *et al.* (1988a) defined area V4 in *Macaca fascicularis* as a single area extending from the dorsal to the ventral surface of the hemisphere and containing the representation of both the inferior and superior quadrants, up to 40° eccentricity. Their study was the first to show a detailed visuotopic organization in area V4. Recently the extent of V4, including a representation of up to 50° eccentricity, both dorsally and ventrally, has been confirmed based on projections from V2 (Gattass *et al.*, 1997).

Therefore, we decided to study the extent and visuotopic organization of area V4 in *Cebus* monkeys using both electrophysiological and anatomical criteria. In addition we submitted our electrophysiological data to bias-free analysis in order to construct maps of the cortical visuotopy. This technique allowed for quantification of certain visuotopic parameters that are not evident by means of analyses based solely on the position of individual receptive fields. Previous accounts of these data were presented elsewhere (Piñon, 1993; Piñon *et al.*, 1993).

Materials and Methods

We used six *Cebus apella* monkeys weighing between 2.5 and 4 kg in anesthetized and paralyzed preparations. Multiunit recordings systematically explored the cortex anterior to V2 with vertical electrode penetrations in chronic preparations. The visual field representation was determined by relating the location of receptive fields of small clusters of neurons to the recording sites in the cortex. Myeloarchitectonic analysis was used to determine the borders of area V4. Biased (manual) and unbiased (computer-generated) maps were constructed to reveal the visual topography in this area, while interpolated and back-transformed maps were used to study its regularity. Quantitative analyses were carried out to reveal the relationships of receptive field sizes and of magnification factor with eccentricity.

Recording Sessions

The experimental procedures for multiunit recordings were described in detail elsewhere (Gattass and Gross, 1981; Gattass *et al.*, 1987; Rosa *et al.*, 1988). Briefly, prior to the first recording session, after the administration of ketamine hydrochloride (Ketalar, Park Davis, 50 mg/kg) and of a benzodiazepinic (Valium, Roche, 2 mg/kg) the animal received a cranial prosthesis. This prosthesis consists of a bolt to attach the head to the stereotaxic apparatus, and a stainless steel recording chamber. The bone inside the chamber was removed, exposing the dura mater. This procedure allows the visualization of main blood vessels and sulci through the dura. These landmarks were used to plan the location of the penetrations. During the recording sessions, anesthesia and analgesia were induced by the administration of Ketalar (25 mg/kg) and Valium (0.5 mg/kg), and the animals were maintained under 70% nitrous oxide/30% oxygen. Muscular paralysis was induced by pancuronium bromide (Pavulon, 0.08 mg/kg/h i.v.). Artificial ventilation was maintained by means of a respiration pump, connected to a tracheal cannula. The level of expired CO_2, the electrocardiogram and the rectal temperature were continuously monitored and kept within physiological range. The eye was fitted with contact lenses, which focused the eye to the surface of a 57.3 cm radius transparent hemisphere placed in front of the animal. The positions of the blind spot and of the fovea were projected onto the hemisphere by means of a reversible ophthalmoscope and used to define the vertical and horizontal meridians of the visual field, as previously described (Gattass and Gross, 1981).

Varnish-coated tungsten microelectrodes with impedance of ~0.5 MΩ at 500 Hz were used to record from small clusters of neurons. Whenever

possible, a single electrode was used in all recording sessions for each animal. Vertical penetrations spaced by 1.0–1.5 mm forming a grid that encompasses area V4 and surrounding areas were made through the intact dura mater. Receptive fields were recorded in steps of 500 μm and small electrolytic lesions were made along the track to help with the precise positioning of recording sites. Under photopic illumination, visual response was elicited by white or colored opaque bi-dimensional or tri-dimensional stimuli, presented onto the surface of a transparent plastic hemisphere, located 57 cm from the center of the eye of the monkey. A contact lens was used to focus the eye onto the surface of the plastic hemisphere (see Gattass and Gross, 1981, for additional details). The accuracy and stability of the eye position during the recording sessions were monitored at intervals by recording the receptive field position in V1 at the opercular surface. The visual topography described here is based on the location of receptive field centers corresponding to 683 recording sites in V4 and surrounding areas, obtained along 211 vertical electrode penetrations in 32 recording sessions, in six animals.

Histological Procedures
The histological procedures were similar to those described by Gattass *et al.* (1987). Briefly, under deep anesthesia (sodium pentobarbital, 50 mg/kg i.v.) the animals were perfused intracardially with saline followed by 4% paraformaldehyde. The brains were then frozen and sectioned in the coronal or parasagittal planes at 40 μm. Sections were stained for cell bodies with cresyl violet or for myelin with a modified Heindenhain–Woelcke method (Gattass and Gross, 1981). The cresyl violet-stained sections were used to reconstruct the penetration tracks and to localize the recording sites while the myelin-stained sections were used to define areal transitions. All electrode penetrations were reconstructed. The recording sites as well as the myeloarchitectonic transitions were transposed onto bidimensional maps of the cortex, constructed as described below.

Unfolding of the Visual Cortex
In order to obtain bidimensional maps of area V4 and surrounding areas for each animal we built three-dimensional wire models of layer IV from sections drawn at 7.5× magnification. These models were then unfolded following the same procedures described by Gattass *et al.* (1987). Discontinuities were introduced in the maps to avoid excessive distortions that would have resulted from the flattening procedure. The recording sites and the myeloarchitectonic borders were projected onto layer IV, orthogonal to the cortical surface, then transposed to the flattened maps.

Definition of borders
The myeloarchitectonic and the electrophysiological transitions were used to define the borders of area V4. The myeloarchitectonic borders were defined at the transitions between two distinct myeloarchitectonic patterns, whereas the electrophysiological borders were defined in regions where reversals of receptive field progressions occurred. The myeloarchitectonic borders had an imprecision of 0.5–1.0 mm and the borders were drawn in the middle of these transitions. The electrophysiological borders had an imprecision of 500 μm due to the sampling method. In all six cases we were able to define the myeloarchitectonic borders. However, we were unable to define all electrophysiological borders in a single case. Therefore, we used different cases to define them. Cases 2 and 3 were used to define the dorsal and ventral borders of V4, while cases 1 and 4 were used to define the dorsal borders, and cases 5 and 6 the ventromedial ones.

Visuotopic Analysis
In order to obtain bias-free visuotopic maps of area V4 for each animal, the location of the recording sites projected on the flattened maps and the corresponding eccentricity and polar angle coordinates of the receptive field centers were digitized. The location of isoeccentricity and isopolar lines were obtained using the interpolation algorithm defined by Maunsell and Van Essen (1987). Briefly, the isoeccentricity and isopolar maps were computed independently by superimposing a 0.25 mm² grid on the cortical map of V4. Line segments were then drawn from each recording site to all bins that were <0.25 mm distant. For each bin of the grid, values of eccentricity and of polar angle were interpolated from lines

that cross it. This way each recording site contributes to all bins within a 0.25 mm radius. Linear scaling was used to interpolate eccentricity and polar angle values. Polar coordinates were interpolated between all possible pairs of recording sites to fill a grid of square bins. The array of bins containing the average value of the coordinate of each bin was used to draw isopolar and isoeccentric lines for each map, as shown in Figures 10–12.

The degree of visuotopic orderliness and the existence of re-representations of sectors of the visual field in V4 were analyzed following the procedures described by Maunsell and Van Essen (1987). An orderly grid corresponding to equally spaced points in the cortex is superimposed upon V4 and back-transformed onto the visual field (Figs 13 and 14). The algorithm used back-transforms the array of interpolated coordinates to nodes of a grid onto the visual field representation. The links between adjacent nodes were preserved during the back-transformation, thereby allowing direct visualization of both topologic and geometric distortions in the visual field representation.

Results
We defined area V4 using combined criteria such as myelo-architecture and electrophysiological mapping techniques. Initially we will show the borders of area V4 defined independently by myeloarchitectural and electrophysiological analyses. Then we will present the locations of receptive field centers used to derive maps of the visual topography based on the traditional method and on computer bias-free methods. We will also show the variations of magnification factor and of receptive field sizes with eccentricity. Finally, we will present interpolated and back-transformed maps which were constructed to evaluate the regularity of the visual topography.

Area V4 forms a continuous belt of cortex from the prelunate gyrus dorsally through the lateral convexity of the hemisphere and the occipito-temporal sulcus ventrally, reaching the vicinities of the calcarine sulcus medially (Fig. 1). V4 is bordered by V3 and V3A posteriorly, by transitional V4 (V4t), posterior inferior temporal cortex (TEO) and temporal ventral posterior area (TVP) anteriorly, and by the dorsal prelunate area (DP) dorsally (Fig. 1). V4 contains a topographically organized representation of 50° of the contralateral hemifield, with the vertical meridian (VM) represented along its posterior border and the horizontal meridian (HM) along its anterior border. The fovea representation in V4 is located laterally, at the tip of the inferior occipital sulcus, and the periphery is represented medially both dorsally and ventrally. The lower quadrant is represented dorsally and the upper quadrant ventrally (Fig. 1). In V4, as in the primary visual area (V1) (Gattass *et al.*, 1987) and in V2 (Rosa *et al.*, 1988) the representation of the central visual field is greatly magnified relative to that of the periphery, so that more than half of its surface is dedicated to the representation of the central 10°. Throughout this paper, the portion of area V4 located between the lunate and the superior temporal sulci on the dorsal surface of the hemisphere will be named dorsal V4 (V4d), while the portion of V4 running ventrally from the inferior occipital sulcus pass the occipital temporal sulcus reaching the vicinities of the calcarine sulcus medially will be named ventral V4 (V4v).

Myeloarchitectural Borders
In sections stained by the Heidenhein–Woelke method, area V4 shows a moderate degree of myelinization and a well-stratified pattern at the infragranular layers. This pattern is observed in central V4d and V4v, but is less conspicuous in peripheral V4. This stratified pattern is characterized by the presence of a pale strip separating the outer from the inner band of Baillarger. The outer band of Baillarger in V4 is prominent and located at mid-thickness in the cortical mantle (Fig. 2A,B).
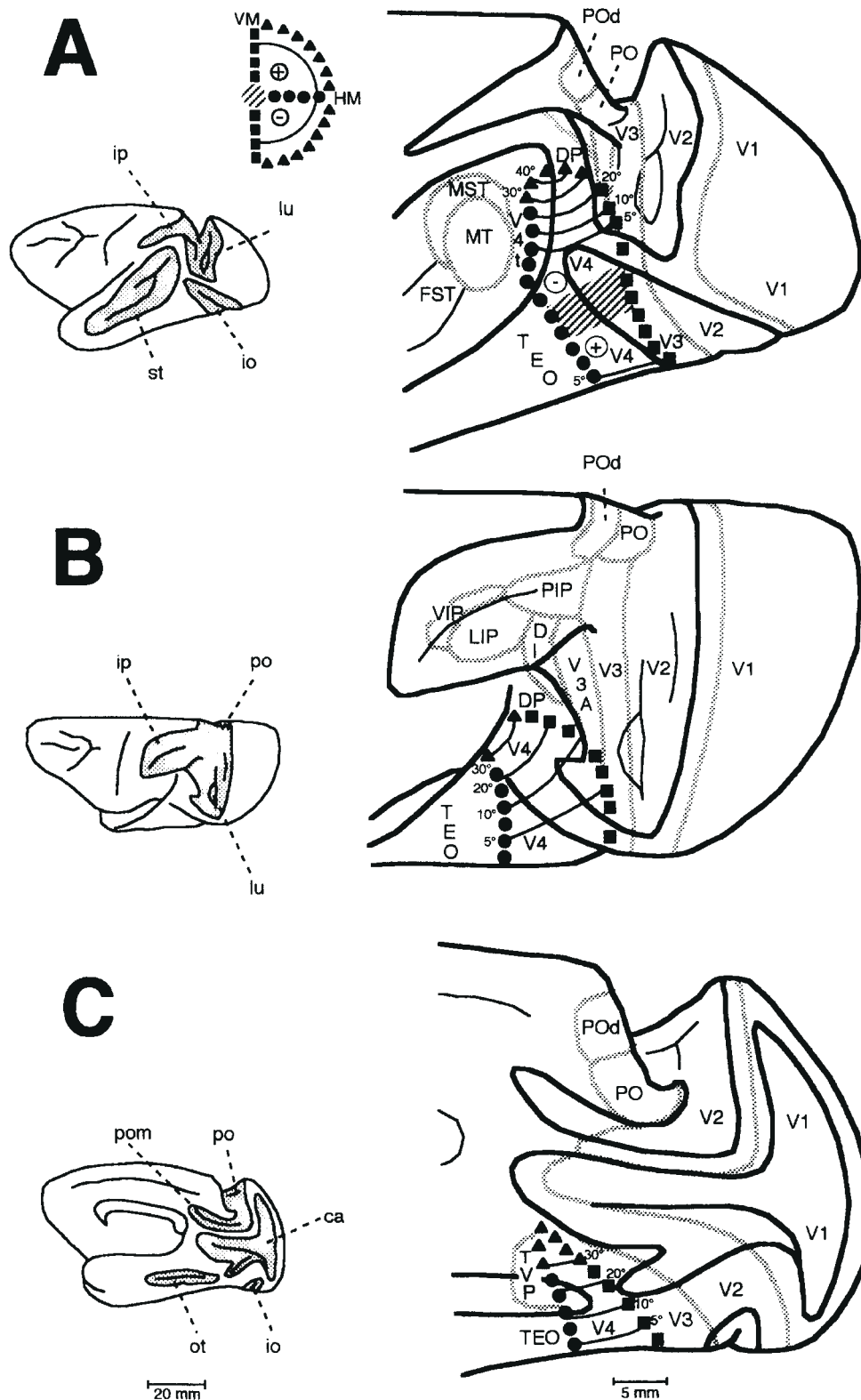
Figure 1. Cortical visual areas and visuotopy of V4 in *Cebus* monkey. Left: lateral (*A*), dorso-medial (*B*) and medial (*C*) views of the cerebral hemisphere with the sulci partially open. Right: enlarged views of the posterior portion of the hemispheres showing the visual areas and the overall topography of area V4 obtained in this study. The filled squares indicate the vertical meridian (VM), the filled circles the horizontal meridian (HM), the filled triangles the periphery and the hatched area the fovea. Thin lines inside V4 represent isoeccentricity lines. Inset: representation of the visual hemifield in polar coordinates. Abbreviations – Sulci: ca, calcarine; io, inferior occipital; ip, intraparietal; lu, lunate; ot, occipitotemporal; po, parietooccipital; pom, medial parietooccipital; st, superior temporal. Areas: DL, dorsolateral; DP, dorsal prelunate; FST, fundus of superior temporal; LIP,lateral intraparietal; MT, middle temporal; MST, medial superior temporal; PIP, posterior intraparietal; PO, parietooccipital; POd, dorsal parietooccipital; TEO, cytoarchitectonic TEO; TVP,temporal ventral posterior; VIP, ventral intraparietal; V1, primary visual area; V2, second visual area; V3, visual area 3; V3A, visual area 3A; V4, visual area 4; V4d, dorsal portion of area V4; V4v, ventral portion of area V4; V4t, transitional V4.
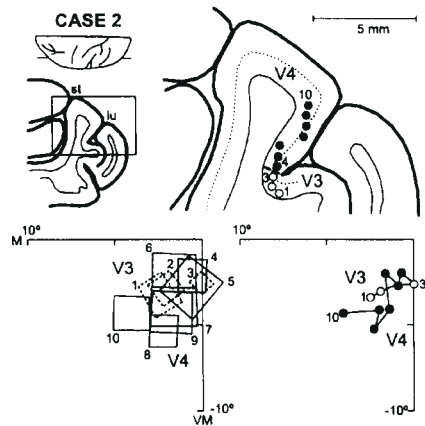
Figure 3. Posterior border of V4d with area V3. Location of receptive fields (lower left) and of receptive field centers (lower right) in dorsal V4 and V3, recorded at the sites indicated in the parasagittal section (upper right) cut at the level indicated in the dorsal view of the brain (upper left). Receptive fields drawn in continuous lines correspond to recording sites in V4 and in dashed lines to recording sites in neighboring areas. From Figures 3–6, filled circles correspond to recording sites in area V4 and open symbols to recording sites in neighboring areas. Dotted line corresponds to layer IV and dashed lines on the section indicate the myeloarchitectonic borders. For abbreviations see Figure 1 legend.

Figure 4. Posterior border of V4d with area V3A. Conventions as in Figure 3. For abbreviations see Figure 1 legend.

Figure 2. Myeloarchitetonic pattern of V4 in two parasagittal (*A,B*) sections of case 1. (*A*) Section corresponding to level C of Figures 7 and 8 illustrates the myeloarchitectonic border between V4d and V3. (*B*) A more medial section, corresponding to level E of Figures 7 and 8, illustrates the myeloarchitectonic borders of both V4d and V4v with surrounding areas. Arrowheads point to borders between V4 and neighboring areas. Multiple arrowheads indicate gradual transitions.

Posterior Borders of V4

Area V3 is located posterior to area V4 except at the dorso-medial regions where V4 is bordered by V3A. V3 is more myelinated than V4 with more compressed infragranular layers. The outer and inner bands of Baillarger in V4 are more conspicuous than in V3. In addition, in V3 the outer band of Baillarger is thinner than in V4, and is also less conspicuous than that of V3A (Fig. 2*B*). V3A is distinguished from V4 by the darker myelination of the infragranular layers as well as by a conspicuous outer band of Baillarger (Fig. 2*B*).

Anterior Borders of V4

Anteriorly, area V4 is bordered by areas V4t dorsally, TEO ventro laterally and TVP (Sousa *et al.*, 1991) ventromedially. Although depicting a defined outer band of Baillarger, V4t can be distinguished from V4 by the heavier myelination of the infragranular layers. In V4t the light band separating the inner from the outer band of Baillarger is not conspicuous (Fig. 2). Similar to V3 there is also a compression of the infragranular layers in V4t. Contrasting with V4, TEO is characterized by a

wider separation between the inner and outer bands of Baillarger and by a heavier myelination of the inner band, which is not well differentiated from the white matter. An undifferentiated inner band and a thin pale outer band of Baillarger characterize TVP. This pattern contrasts with the conspicuous bi-stratified pattern of V4 (Fig. 2*B*).

Dorsomedial Border of V4

Dorsomedial to area V4 we found a region with a distinct myeloarchitectonic pattern that we named DP, following the nomenclature suggested by Andersen *et al.* (1990). This area can be distinguished from V4 by the presence of a sharp outer band
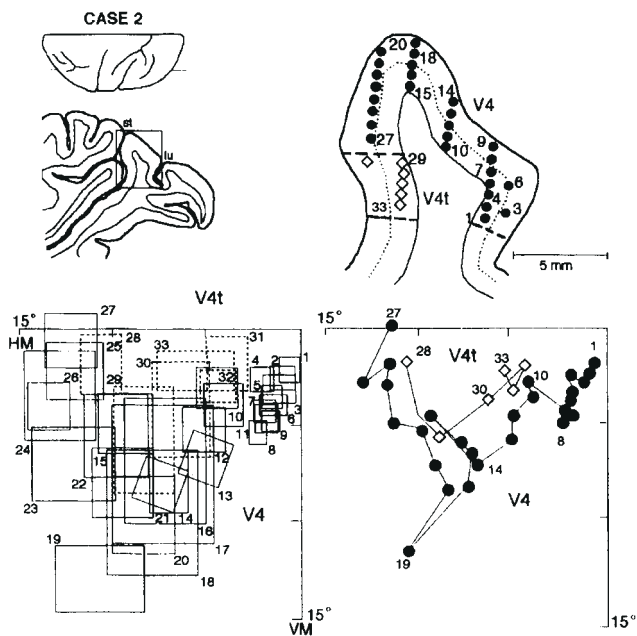
Figure 5. Anterior border of V4d with area V4t. Conventions as in Figure 3. For abbreviations see Figure 1 legend.

Figure 6. Anterior border of V4v with area TEO Conventions as in Figure 3. For abbreviations see Figure 1 legend.

of Baillarger and by the homogeneous aspect of the infragranular layers. In addition, area DP has clear radial bundles of fibers, not visible in V4.

Electrophysiological Borders

Abrupt changes in the progression of receptive field centers in the visual field corresponding to sites located sequentially in the cortex, as well as changes in receptive field sizes, were used as independent criteria to define the borders of V4. For the precise determination of the extent of V4 we took into consideration both the electrophysiologically as well as the myeloarchitectonically defined borders.

Dorsally, the posterior border of V4 with both V3 (Fig. 3) and V3A (Fig. 4) coincides with a reversion in the sequence of receptive field centers at the vertical meridian in the lower quadrant as well as with an increase in receptive field sizes.

The anterior border of area V4d with V4t corresponds to a reversal of receptive fields sequence at the representation of the periphery (Fig. 5). Dorsomedially, anterior to V3A, V4d borders another region, which contains the inferior quadrant of the visual field. This region has large receptive fields and may include more than one visual area. This area was considered as area DP, inasmuch as it coincides in location and in receptive-field size with area DP of *Macaca* as described by Andersen *et al.* (1990). This border is characterized by a reversion or disruption in the sequence of receptive field centers at peripheral portions of the visual field and by a marked increase in receptive field sizes from area V4 to DP.

Ventrally, the posterior border of V4v with V3 coincides with a reversion in the sequence of receptive field centers at the vertical meridian, in the upper quadrant. This reversion is also accompanied by an increase in receptive field sizes. Anteriorly, V4v borders area TEO at more lateral levels and area TVP medially. The border of V4v with area TEO corresponds to the representation of the central horizontal meridian (Fig. 6), while the border between V4v and TVP is topographically incongruent. At this border there is a discontinuity in the sequence of
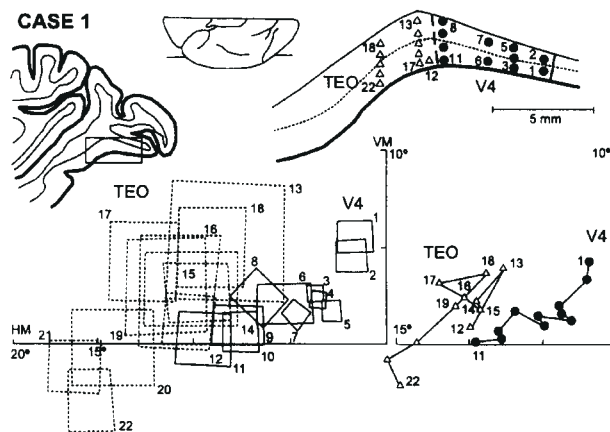
receptive field centers jumping from the horizontal meridian to the periphery. This is also accompanied by a larger increase in receptive field sizes (not illustrated).
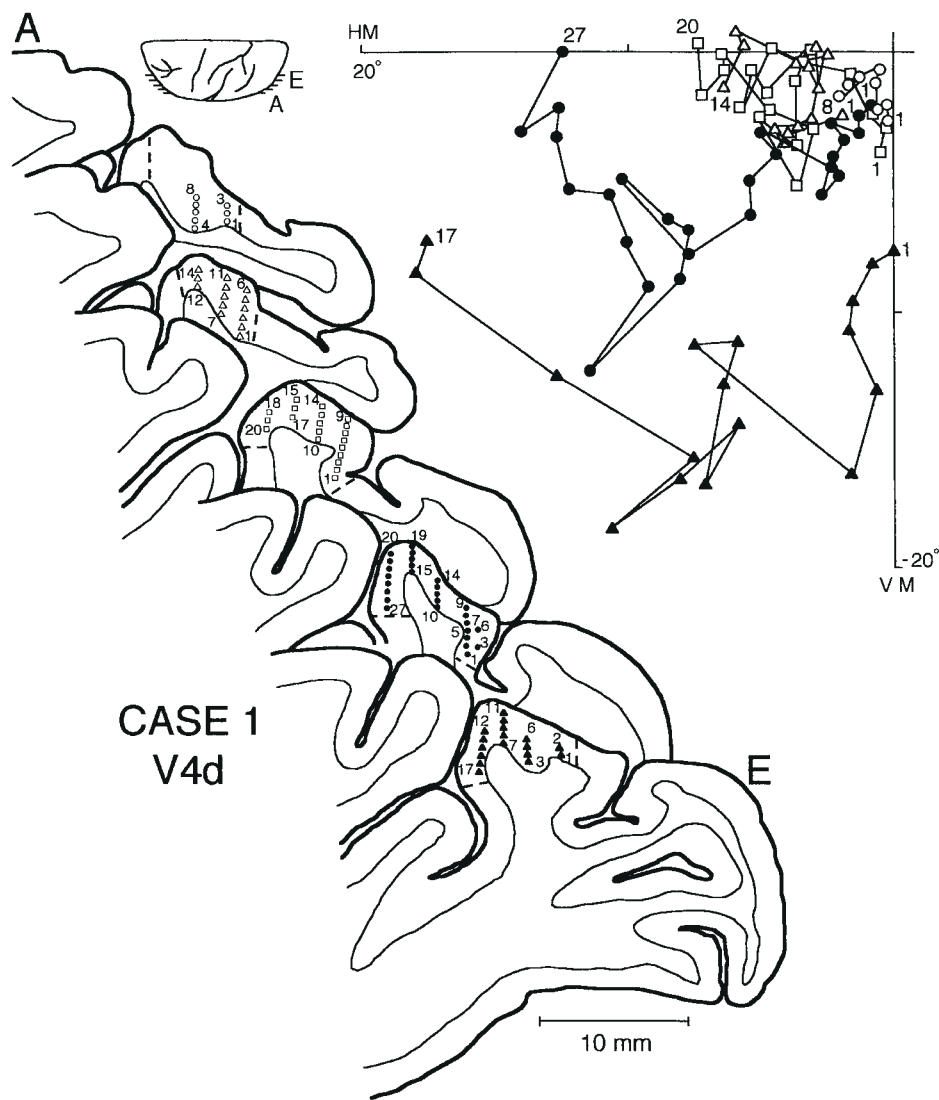
Visuotopic Organization

Figures 7 and 8 illustrate receptive field centers and corresponding recording sites in parasagittal sections of one animal for both V4d and V4v (case 1). These figures show that the lower quadrant is represented dorsally (Fig. 7), while the upper quadrant is represented ventrally (Fig. 8). In addition, the central portion of the visual field is represented laterally, while the peripheral portion is represented medially, both dorsal and ventrally. The representation of the central visual field is magnified relative to that of the periphery (see also Figs 9 and 17).

At more lateral sections, sequences of recording sites from posterior to anterior, in V4, correspond to receptive field centers that progress in the visual field from the representation of the vertical meridian to that of the horizontal meridian. At more medial levels, however, they progress towards the periphery. In Figure 8, the receptive field centers corresponding to recording sites in section E represent more peripheral portions of the visual field than those in section F, which are located more medially. This can be explained based on the fact that recording sites in section F do not extend as far anteriorly as do those in section E.

Figure 9 illustrates the overall visuotopic organization of V4 in a two-dimensional reconstruction of prestriate cortex based on data from case 1. In V4 the foveal region is represented laterally, the lower quadrant dorsally and the upper quadrant ventrally. The vertical meridian corresponds to the posterior border, while the horizontal meridian is represented at its anterior border (Fig. 9*B*) The isoeccentricity lines run from the vertical to the horizontal meridian (Fig. 9*C*), while the isopolar lines run dorsoventrally, in an orientation almost parallel to the meridians (Fig. 9*D*).

Bias-free Visuotopic Organization of V4

Data from four of the animals included in this study were submitted to an automatic computer analysis to generate bias-free visuotopic maps of area V4. In spite of interanimal variability and in differences in sampling, a similar visuotopic organization was observed in all cases. Two of these cases are illustrated in Figures 10–12. These figures show bidimensional maps of V4 with interpolated coordinates for cases 1 and 2. The

Figure 7. Visuotopic organization of V4d in case 1. Location of receptive field centers corresponding to recording sites in V4d indicated on parasagittal sections (*A–E*) cut at the levels indicated on the dorsal view of the brain (upper inset). Different symbols were used for each section. For abbreviations see Figure 1 legend.

visuotopic maps thus obtained are comparable to those described in the previous section (compare Fig. 9 with Figs 10 and 11).

Regularity of the Visuotopic Organization in V4

Analysis of our data showed local irregularities in the representation of the visual field within V4 (see Figs 7 and 8). In order to systematically evaluate the disorderliness in the visuotopic organization of V4 we submitted the data to a bias-free computer analysis. The interpolated data were used to construct back-transformed maps that enable us to evaluate the degree of local re-representations in the visual field. Back-transformed maps for two different cases (cases 1 and 2) are shown in Figures 13 and 14. As was previously stated (Schwartz, 1980; Van Essen *et al.*, 1984; Maunsell and Van Essen, 1987; Fiorani *et al.*, 1989), a precisely organized cortical map transforms a square grid in the cortex onto an orderly cobweb pattern in the visual field. However, in V4, the back-transformed maps obtained revealed distortions in this grid, which shows superimposed domains that suggest a coarse representation, with small local re-representations of parts of the visual field. In addition, a close analysis

of these back-transformed maps also suggests that V4d is more organized than V4v.

Extent of Visual Field Representation in Area V4

The contours of receptive fields recorded in all cases in this study show that area V4 has an almost complete representation of the binocular visual field with a small invasion of the ipsilateral visual field (Fig. 15). V4d contains a representation of 50° of the inferior quadrant, while V4v has a representation that extends up to 60° in the superior quadrant. The portions of the visual field represented in dorsal and ventral V4 are complementary to each other, although V4v shows a small invasion of the inferior quadrant, of ~5°. Due to the nature of the receptive field sampling with vertical penetrations in the cortex, it is likely that more peripheral receptive fields could be recorded in the small, unsearched peripheral portions of V4. Thus, we cannot rule out the possibility of V4 having a virtually complete representation of the binocular visual field.

Receptive Field Size

Multiunit receptive field size (RFS), defined as the square root of
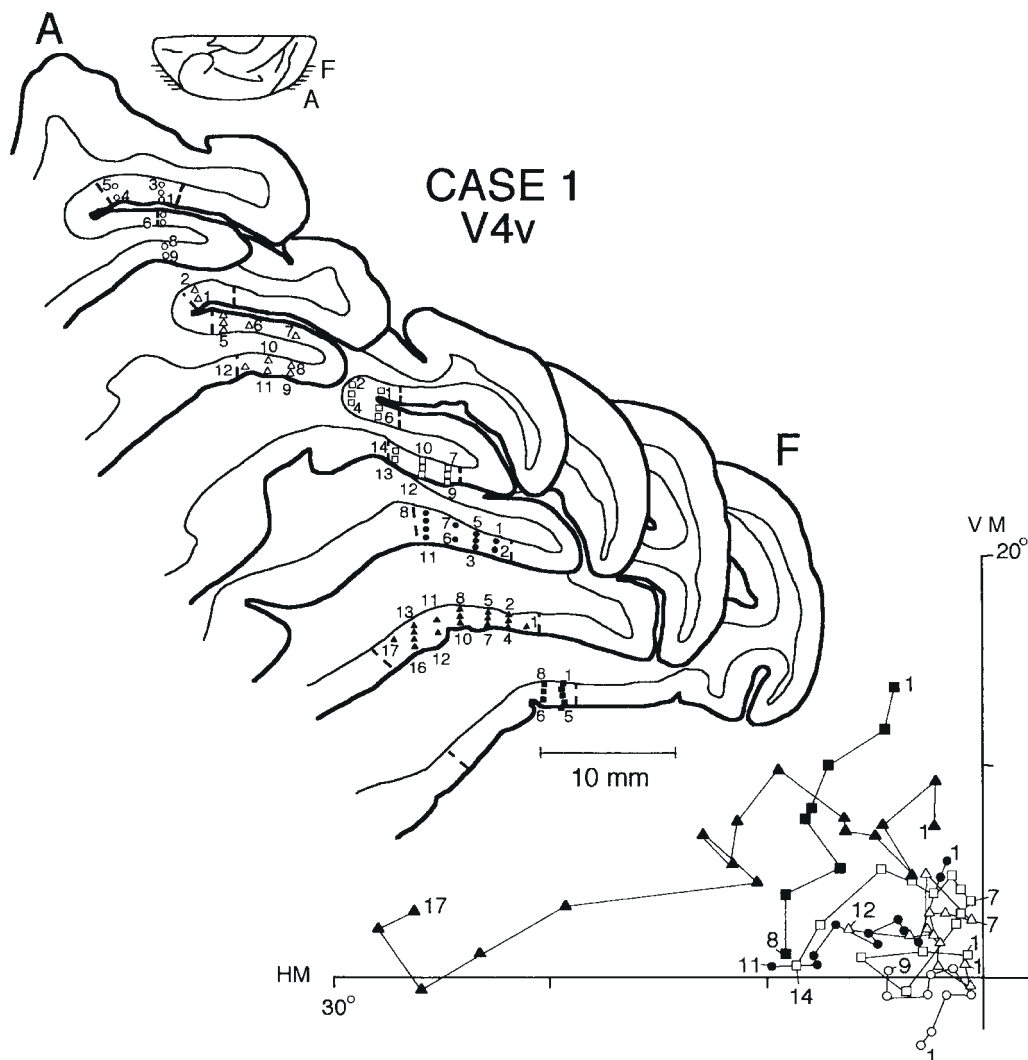
Figure 8. Visuotopic organization of V4v in case 1. Location of receptive field centers corresponding to recording sites in V4v indicated on parasagittal sections (*A–F*) cut at the levels indicated on the ventral view of the brain (upper inset). Different symbols were used for each section. For abbreviations see Figure 1 legend.

receptive field area, increases with increasing eccentricities. Figure 16 shows this variation based on data pooled from four animals. The variations of receptive field size with eccentricity in dorsal and ventral V4 are similar ($P < 0.01$). In order to compare this variation with that of other visual areas, a straight line and a power function were fitted to the pooled data by the method of least squares. Analysis of Figure 16 shows that the straight line (RFS = 0.4 + 0.31 ecc) fits the data best.

Cortical Magnification Factor

The variation of cortical magnification factor (CMF), i.e. the ratio of the cortical distance between two recording sites (in millimeters) and the distance, in degrees, between the corresponding receptive field centers (Daniel and Whitteridge, 1961), was determined as a function of eccentricity. This evaluation was performed with the aid of an automatic system, which calculates CMF by using all possible pairs of recording sites from digitized flattened maps of layer IV of area V4. The cortical magnification factor was determined along the isopolar as well as along the isoeccentric dimensions for V4d and V4v independently (Fig. 17). It can be seen in this figure that overall CMF decreases with increasing eccentricities. In V4d, CMF

varies as a function of eccentricity by a power function with an exponent of –0.82 (correlation coefficient, $r = 0.6$) along the isoeccentric domain and with an exponent of –0.71 ($r = 0.6$) along the isopolar domain. In V4v, CMF also varies with eccentricity with an exponent of –0.6 for the isoeccentric domain ($r = 0.5$) and of –0.3 for the isopolar one ($r = 0.3$). The differences in the regressions for V4d and V4v were not statistically significant.

Anisotropy

During the course of the magnification analysis, a difference between the isoeccentric and isopolar magnification was detected. Therefore, a *t*-test was performed to evaluate whether these differences were significant. The presence of significant differences would imply the existence of anisotropies in the visual field representation in V4. The result of this analysis pointed to heterogeneous differences in the sample. Some cases presented higher isoeccentric magnifications than isopolar ones, while others showed higher isopolar magnifications. The signal-to-noise ratio in this analysis was high. Thus, we proceeded to evaluate the anisotropies on the bidimensional maps by measuring, directly on these maps and on the visual field, the distance between two isopolar and two isoeccentric lines within
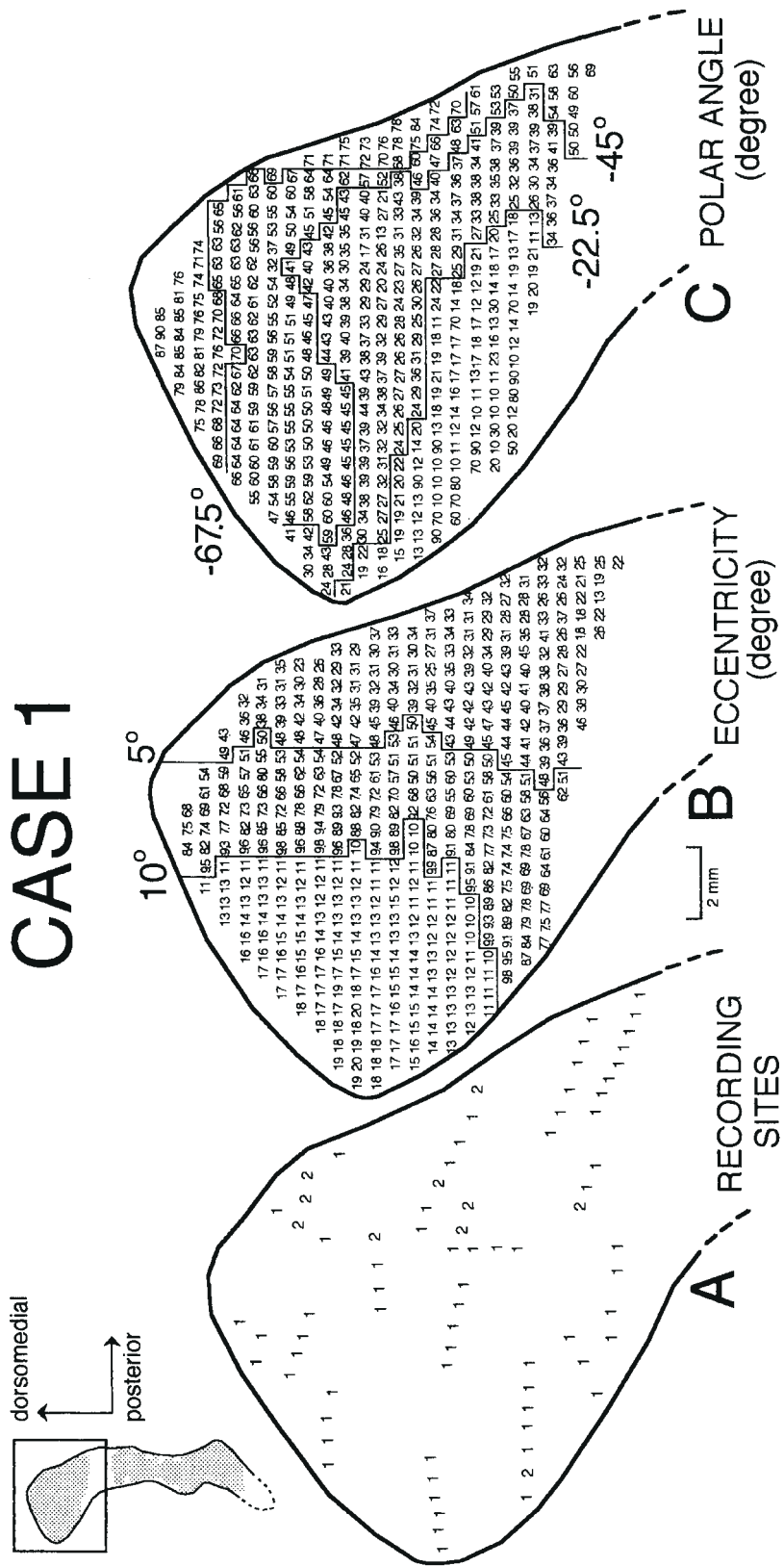
CASE 1
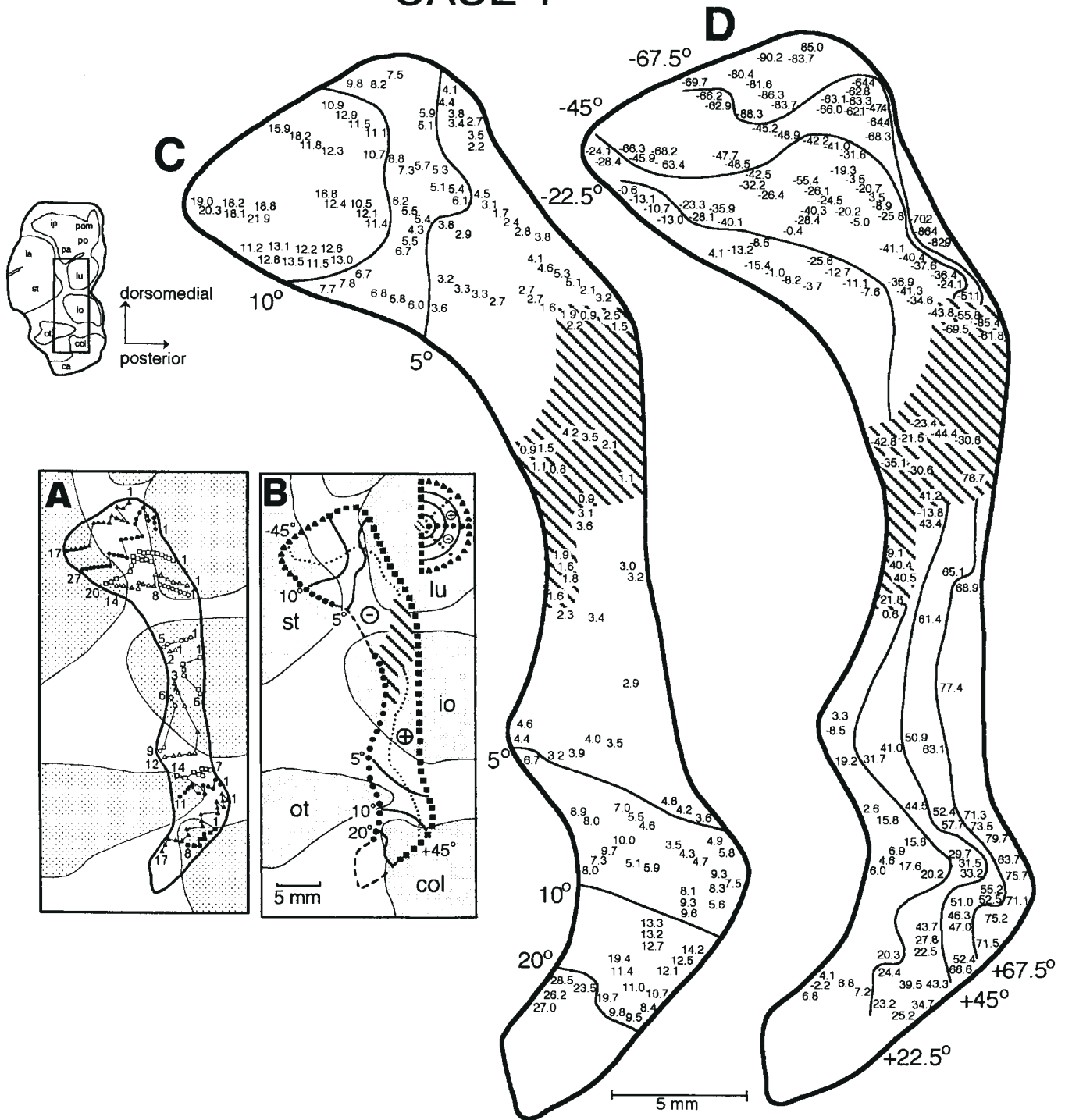
Figure 9. Overall visuotopic organization of V4 illustrated on a flattened map of pre-striate cortex. (*A*) Recording sites sequences illustrated in a portion of the flattened map of pre-striate cortex (box in inset). The recording sites correspond to receptive field centers illustrated in Figures 7 and 8, with the same symbols. (*B*) Visuotopic map of V4. (*C*) Eccentricity values of the receptive field centers illustrated in (*A*). These values were used to determine the location of isoeccentricity lines. (*D*) Isopolar values of the receptive field centers illustrated in (*A*). These values were used in the determination of isopolar lines. Hatched area: foveal representation. For abbreviations see Figure 1 legend.

the same sector of the visual field. The ratio of these two values was called the anisotropy index. Figure 18 shows an example of how the anisotropy index was obtained for each sector of the visual field. The anisotropy indices thus obtained suggest

the existence of differences in the relationship between iso-eccentric and isopolar lines in the cortex and in the visual field. This difference is present throughout central and peripheral V4 (Fig. 19).

Figure 10. Bias-free map of V4d (case 1). Flattened maps of the dorsal portion of V4 (box in inset) showing interpolated eccentric values with derived isoeccentric lines (*B*) and polar values with isopolar lines (*C*). In (*A*) the numerals represent the number of recording sites in each bin.
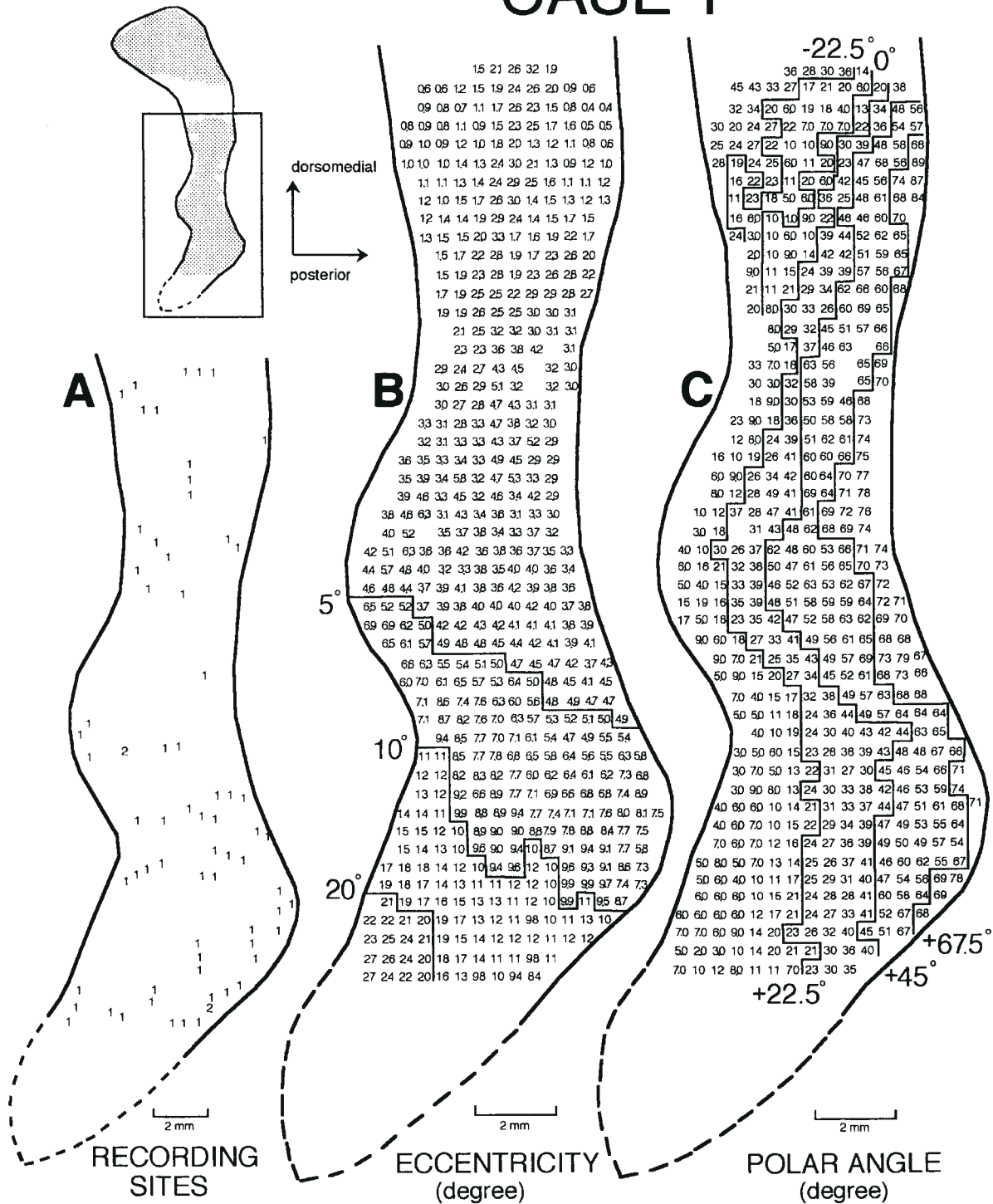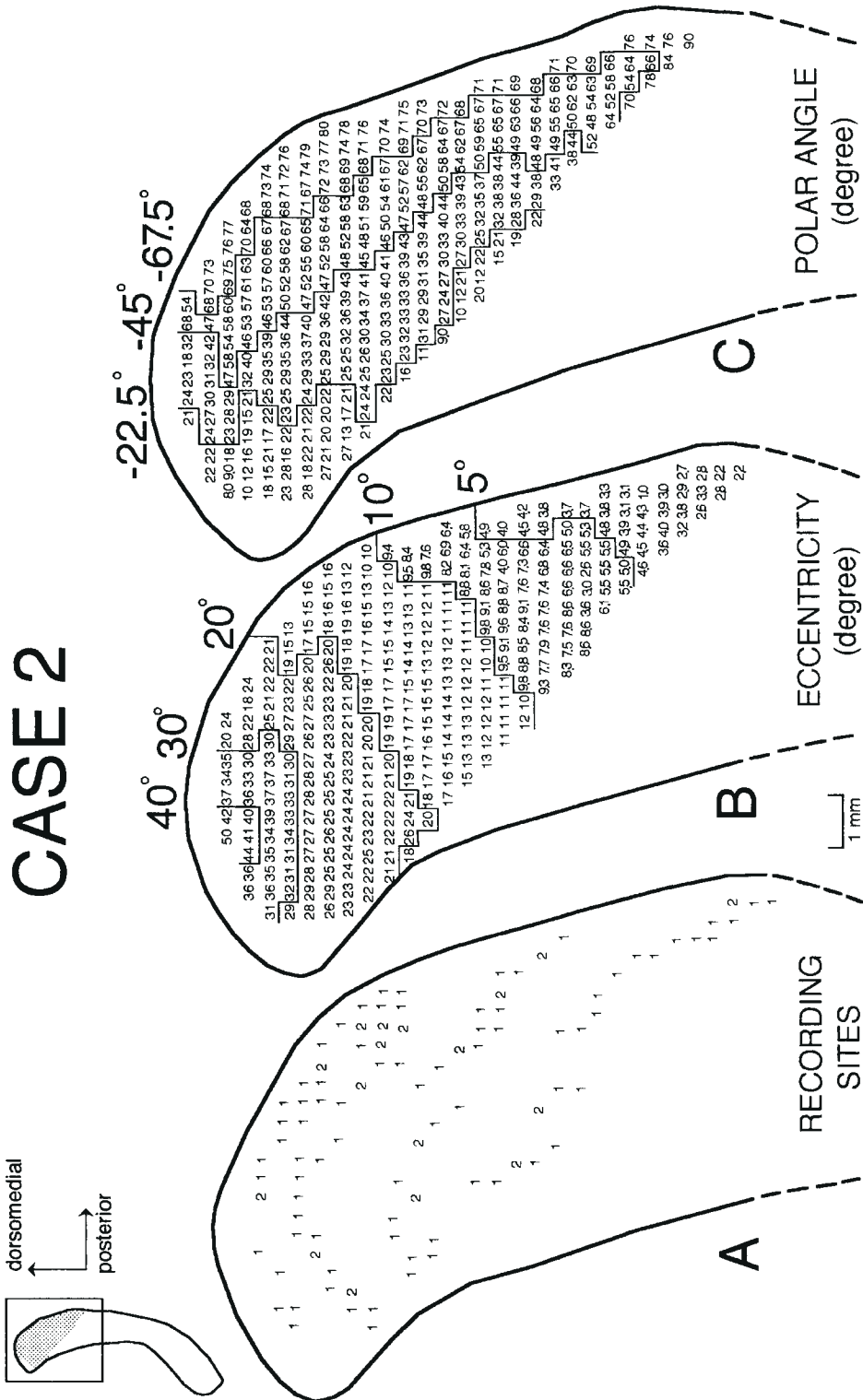
CASE 1

A — RECORDING SITES

B — ECCENTRICITY (degree)

C — POLAR ANGLE (degree)

dorsomedial

posterior

5° 10° 20°

-22.5° 0° +22.5° +45° +67.5°

2 mm

Figure 11. Bias-free map of V4v (Case 1). For details see Figure 10 legend.

Discussion

Area V4 was first thought to have only a restricted quadrantic visuotopic organization (Zeki, 1971; Van Essen and Zeki, 1978; Maguire and Baizer, 1984). Subsequent studies characterized V4 as a large area containing an almost complete representation of the hemifield (Gattass et al., 1988a). In the present work we describe area V4 in *Cebus* as a continuous strip of cortex, extending from the dorsal to the ventral aspects of the hemisphere. The results here described also confirm those of a previous study in *Cebus,* based on anatomical connections (Piñon et al., 1990; Sousa et al., 1991) and are also comparable with those of area V4 defined in *Macaca* based on electrophysiology (Gattass et al., 1988a) as well as on anatomical connections with area V2 (Nakamura et al., 1993; Gattass et al.,

Figure 12. Bias-free map of V4d (Case 2). For details see Figure 10 legend.
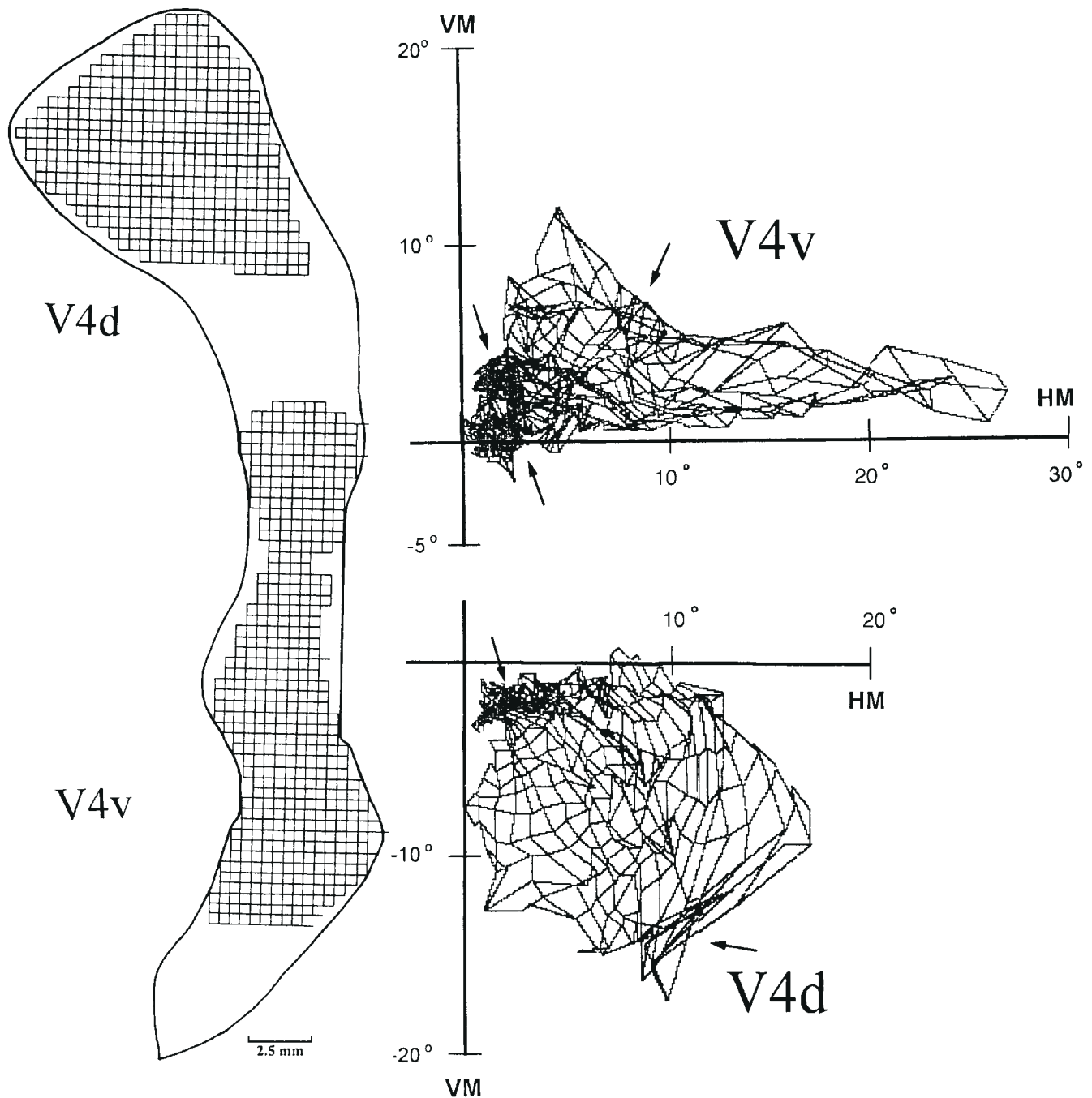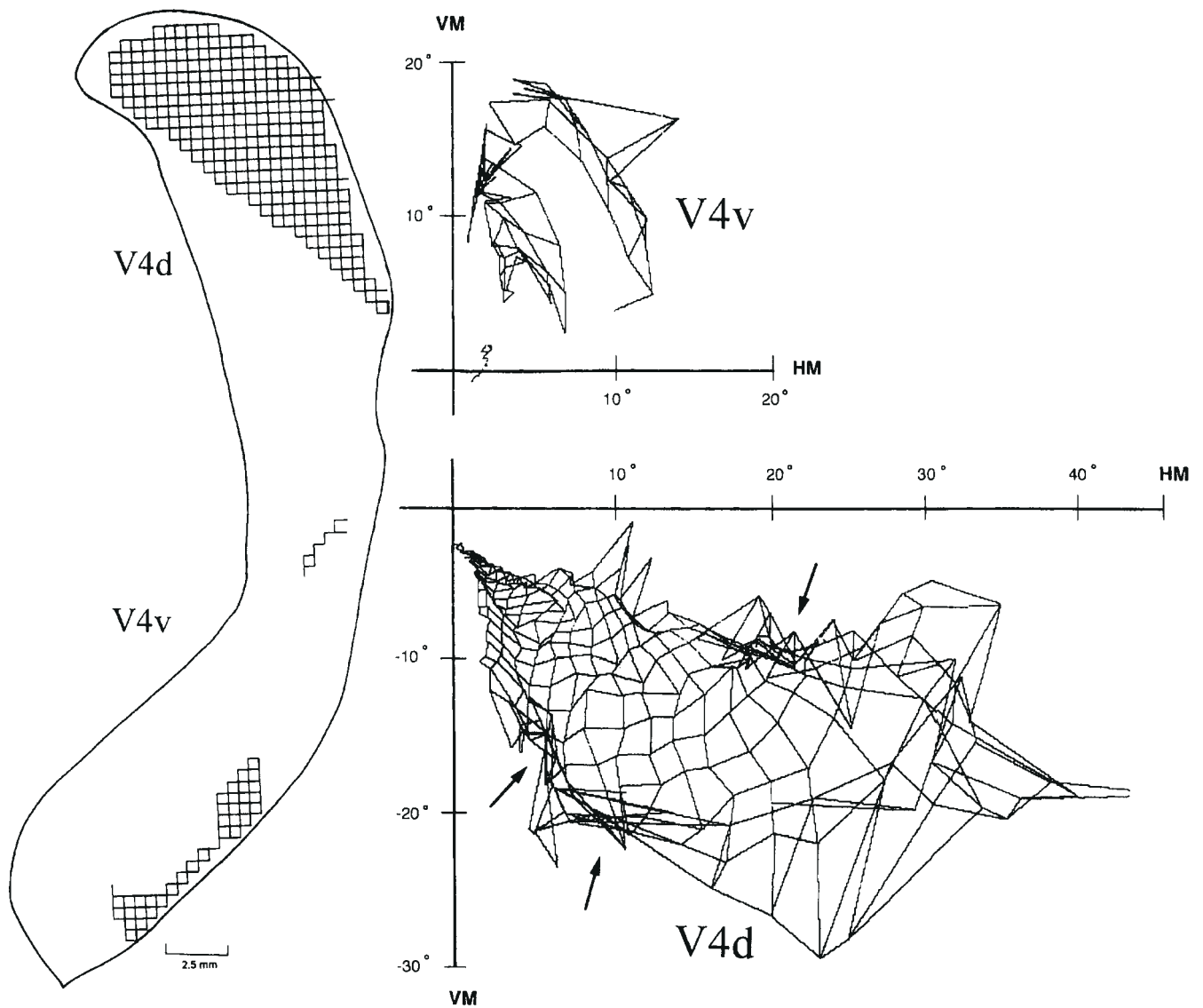
Figure 13. Back-transformed maps of V4 (case 1). Imaginary grids spaced by 0.25 mm on the cortical surface were back-projected onto the representation of the visual hemifield (right) at the corresponding values of the interpolated coordinates. Note that V4d represents lower visual field, while V4v represents upper visual field. Arrows point to local re-representations of the visual field. For abbreviations see Figure 1 legend.

1997). The extent and visuotopic organization of area V4 in macaque monkey (Gattass *et al.*, 1988a) has been accepted by several authors (Desimone and Ungerleider, 1986; Boussaud *et al.*, 1991; Felleman and Van Essen, 1991; Van Essen *et al.*, 1992; Nakamura *et al.*, 1993; Van Essen and Gallant, 1994) and disputed by others (Zeki, 1971, 1978, 1993, 1996; Van Essen and Zeki, 1978; Maguire and Baizer, 1984; Youakin and Baizer, 1990; Stepniewska and Kaas, 1996). Interestingly, although V4 had been defined as a target of V2 (Zeki, 1971), the pattern of connection with this area had not been used to determine V4

extent. Recently Gattass *et al.* (1997) demonstrated the existence of a representation of the periphery extending to 50° eccentricity in area V4, similar to the results of the present paper.

Visual Topography
Our data showed that area V4 has an almost complete representation of the binocular visual field, with the upper quadrant represented ventrally and the lower quadrant dorsally. Unlike V2 and V3 (Gattass *et al.*, 1988b; Rosa *et al.*, 1988), the dorsal and ventral segregation in V4 does not respect the horizontal

Figure 14. Back-transformed maps of V4 (case 2). See also legends to Figures 1 and 13.
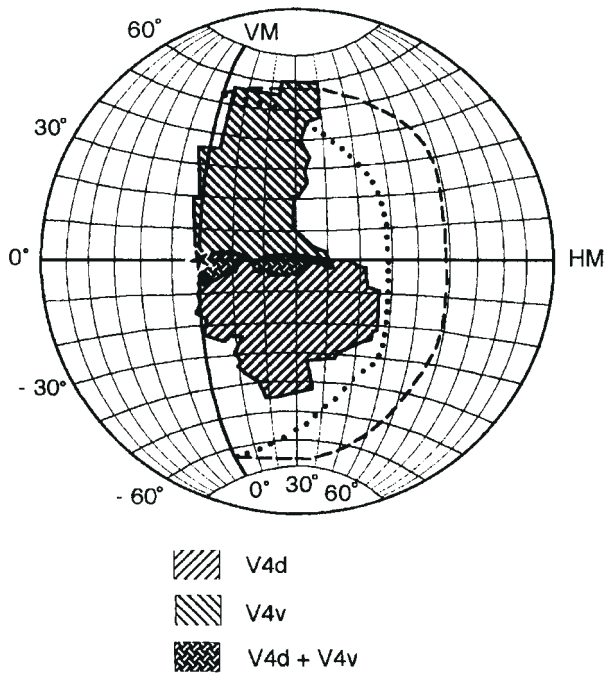
meridian, rather a small portion of the inferior visual field, ~5°, is represented on the ventral surface. An invasion of the inferior visual field representation on the ventral surface has been described for area DL in the owl monkey (Allman and Kaas, 1974).

The visuotopy of V4 is cruder than that found in areas V1, V2, V3 and MT in *C. apella* (Gattass *et al.*, 1987, 1988b; Rosa *et al.* 1988; Fiorani *et al.* 1989) The distribution of isoeccentric and isopolar lines in V4 demonstrated a well-organized visuotopy along the isoeccentric lines similar to areas V2 and V3 (Gattass *et al.*, 1988b; Rosa *et al.*, 1988) and different from the parieto-occipital (PO) and dorsal parietooccipital areas (POd) in *Cebus* (Neuenschwander *et al.*, 1994). The back-transformed maps of the visual field represented in area V4 show a large scatter in this area as compared with areas V1, V2, V3 and MT of *Cebus* monkey (Gattass *et al.*, 1987, 1988b; Rosa *et al.*, 1988; Fiorani *et al.*, 1989). This could be related to the large sizes of receptive fields in V4 inasmuch as it has been shown that the scatter in the visuotopic organization of both V1 and MT of *Macaca* is
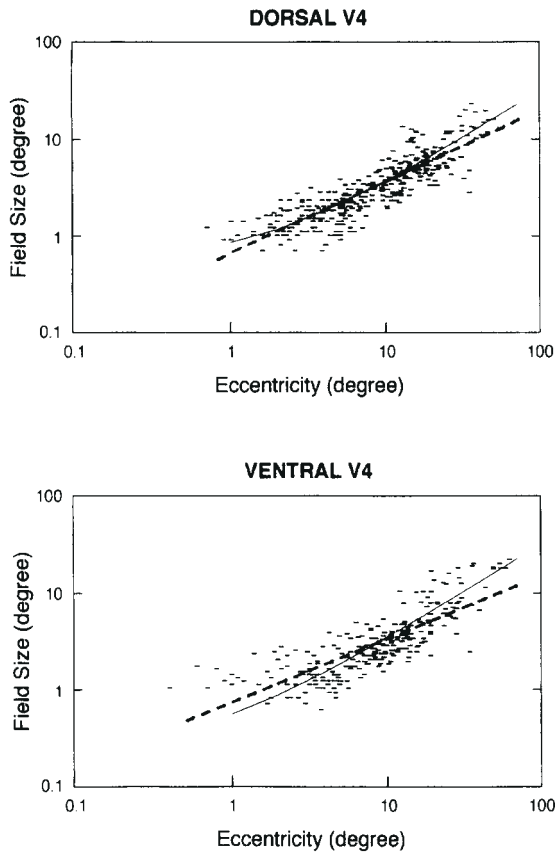
proportional to receptive field sizes (Hubel and Wiesel, 1974; Gattass and Gross, 1981). It could also be due to the variety of inputs, including those from visuotopically organized areas (V2 and V3), crudely visuotopic organized area (TEO) and non-visuotopically organized area (inferior temporal cortex).

The fact that more than half of V4 is devoted to the first 10° of the visual field with the remaining of the visual field, up to 50°, compressed in few millimeters at the medial portions of V4 rendered it difficult to record from this portion of the area. This could account for the few recording sites in this region and for a possible underestimation of the extent of the visual field represented in V4.
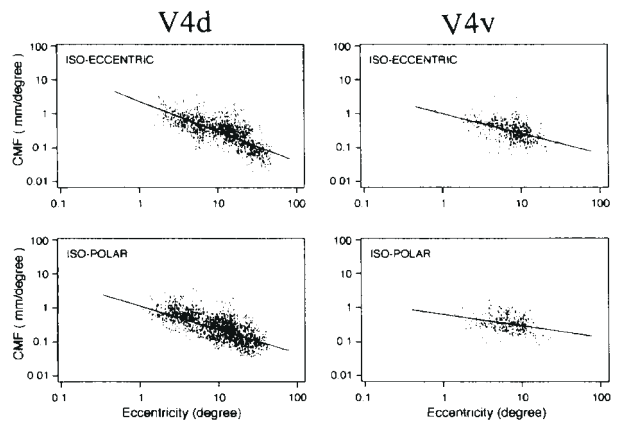
In *Cebus,* cortical magnification factor values are similar to those found for *M. fascicularis* (Gattass *et al.*, 1988a). This type of visuotopic organization is consistent with the visuotopy of areas of the ventral stream, differing from those of the dorsal stream (Ungerleider and Mishkin, 1982; Gattass *et al.*, 1990; Baizer *et al.*, 1991; Van Essen and Gallant, 1994). Comparisons between the values for cortical magnification factors obtained

Figure 17. Cortical magnification factor (CMF) as a function of eccentricity in V4. Data pooled from the six cases used in this study. Cortical magnification factor along the isoeccentric (upper) and isopolar (lower) dimensions are illustrated separately for V4d (left) and V4v (right). See text for details.
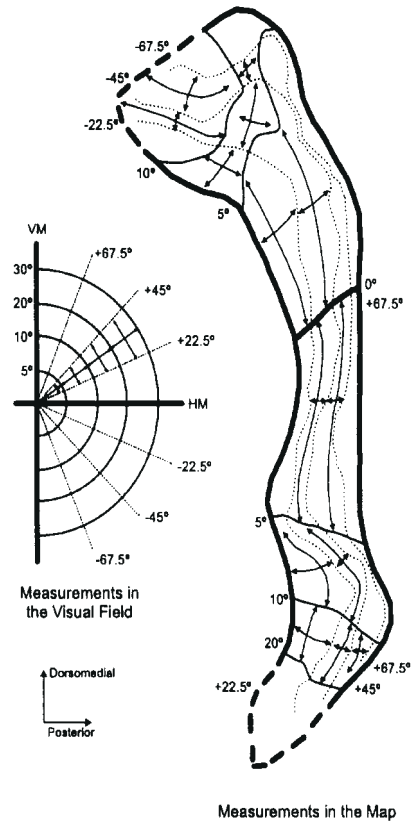

Figure 15. Extent of the visual field represented in V4 based on data pooled from all cases studied. Dashed line represents the extent of the monocular visual field while the dotted line represents the binocular visual field in *Cebus* monkey. Star represents the center of gaze. For abbreviations see Figure 1 legend.

Figure 18. Schematic diagram of manual measurements of anisotropy in area V4. Thinner lines represent isoeccentric lines while dotted lines represent isopolar ones. Arrows represent the dimensions along the isoeccentric and isopolar domains. Left: Cartesian coordinates showing the domains measured using the same symbols. See text for details.

Figure 16. Receptive field size as a function of eccentricity in V4. Data pooled from the six cases included in this study. The power (dashed lines) and linear (continuous lines) functions were fitted to the data by the method of least squares. See text for details.

along the isopolar and isoeccentric lines suggest the existence of anisotropy in the representation of the visual field in both ventral and dorsal V4 being 1.5–2.0 times greater along the isopolar lines. Anisotropies in the representations of the visual field have already been described for other areas in *Cebus* (V1: Gattass *et al.*, 1987; V2: Rosa *et al.*, 1988; ventral V3: Gattass *et al.*, 1988b)
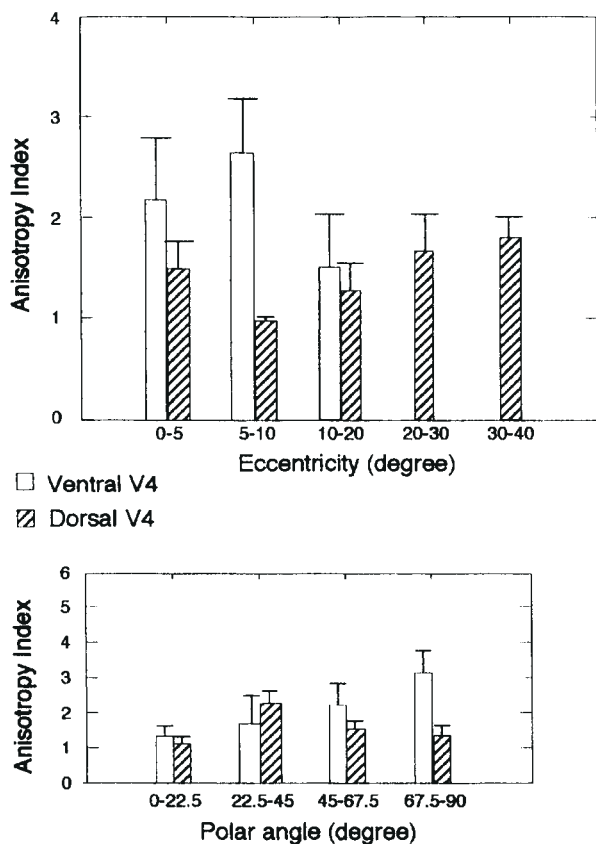
Figure 19. Anisotropy indices in V4. Histograms show the anisotropy indices as a function of eccentricity for V4d and V4v. Measurements were made along the isoeccentric (upper) and isopolar (lower) domains.

as well as for some areas in *Macaca fascicularis* (VP: Fenstmaker *et al.*, 1986; Newsome *et al.*, 1986; V2: Roe and Ts'o 1995).

Two distinct modules have been described in V4 (Zeki and Shipp, 1989; Van Essen *et al.*, 1990; DeYoe and Sisola, 1991). These types of compartments could be involved in the two major streams of visual processing, inasmuch as V4, which was initially described as participating only in the ventral stream, has recently been demonstrated to participate also in the dorsal one (Maunsell *et al.*, 1990; Morel and Bullier, 1990; Baizer *et al.*, 1991; Ferrera *et al.*, 1991, 1992; Nealey *et al.*, 1991). Using a combination of *in vivo* optical imaging, electrophysiology and anatomical injections in the prelunate gyrus, Ghose and Ts'o (1997) described a collection of overlapping and interacting modules for orientation, color and size inside area V4. Thus one could postulate that the anisotropy found in V4 could reflect the presence of these modules inside this area.

Comparison with Other Primates

It has been suggested that V4 is homologous to the dorsolateral area (DL) described in *Aotus* (Weller and Kaas, 1985; Kaas and Krubitzer, 1991). However, DL is an area restricted to the dorsal aspect of the hemisphere, while our results show that area V4, in *Cebus*, is a strip of cortex that extends further ventrally, reaching the temporal lobe. Along the antero-posterior dimension, area DL has been initially subdivided into two areas: caudal DL (DLc) and rostral DL (DLr) (Cusik and Kaas, 1988; Kaas and Morel, 1993; Stepniewska and Kaas, 1996). More recently, Sereno and Allman (1990) and Sereno *et al.* (1994),

using electrophysiological data, described three areas located between V2 and MT: posterior DL (DLp), intermediate DL (DLi) and anterior DL (DLa). Based solely on the location of the areas, we suggest that DLp may correspond to V3d (Gattass *et al.*, 1988a), to PM (Maguire and Baizer, 1984) or to DLc (Stepniewska and Kaas, 1996) as described in *Macaca*. DLi may correspond to dorsal V4 described in *Cebus* (present data) as well as to V4d (Gattass *et al.*, 1988a), to DLr (Stepniewska and Kaas, 1996) or to AL (Maguire and Baizer, 1984) in *Macaca*. DLa may correspond to area V4t of both *Cebus* (present data) and *Macaca* (Desimone and Ungerleider, 1986). In the owl monkey, Sereno *et al.* (1994) proposed the existence of two upper quadrant representations anterior to V2 in the ventral surface, which they named ventro-posterior (VP) and ventro-anterior (VA) areas. In the macaque an upper quadrant representation, immediately anterior to V2, has also been described. This region has been named as VP by Burkhalter *et al.* (1986) and by Newsome *et al.* (1986), and as V3v by Gattass *et al.* (1988a). In addition, Gattass *et al.* (1988a) described an upper field representation in V4, in the ventral surface, that could be homologous to VA described by Sereno *et al.* (1994) in the owl monkey. In a review on the organization of extrastriate cortex, Rosa (1997) suggested that the main differences between New and Old World monkeys are in the definition of the dosolateral cortex, between V2 and V4t. In fact, our data in *Cebus* (present study; Gattass *et al.*, 1988b; Sousa *et al.*, 1991) suggest that the lower-quadrant representations found in dorsal V3 and V4 could correspond to areas PM and AL defined in the dorsolateral cortex of macaques by Maguire and Baizer (1984). Therefore PM and VP are likely to correspond to V3 inasmuch as together they contain a complete representation of the visual field anterior to V2. In addition, AL and VA, which together form another representation, may correspond to V4.

Area V4 in *Cebus* resembles that of the macaque in extent and position relative to other areas. They also have similar myeloarchitectonic characteristics. These results, together with those of other visual areas in *Cebus* monkey (Gattass *et al.*, 1987, 1990; Rosa *et al.*, 1988; Fiorani *et al.*, 1989; Sousa *et al.*, 1991; Piñon, 1993; Piñon *et al.*, 1993; Rosa *et al.*, 1993; Neuenschwander *et al.*, 1994), point to a similarity in the organization of visual areas of *Cebus* and *Macaca*. This similarity could be attributed to factors such as the sizes of the brain and of the animal (Fleagle, 1988), sulcal pattern (Le Gros Clark, 1959), diurnal behavior and a rich repertoire of hand manipulation.

Recently, several studies in human using functional magnetic resonance imaging have described the retinotopic organization of different visual areas (Sereno *et al.*, 1995; DeYoe *et al.*, 1996; Tootell *et al.*, 1996). Anterior to area VP, Sereno *et al.* (1995) showed a representation of the upper visual quadrant corresponding to V4v. Dorsally, anterior to area V3, they found upper and lower visual field representations, which may correspond to areas V3A and V4d described in monkeys (Gattass *et al.*, 1988a; present study).

References

Allman JM, Kaas JH (1974) A crescent-shaped cortical visual area surrounding the middle temporal area (MT) in the owl monkey (*Aotus trivirgattus*). Brain Res 81:199–213.

Andersen RA, Asanuma, C, Essick G, Siegel RM (1990) Corticocortical connections of anatomically and physiologically defined subdivisions within the inferior parietal lobule. J Comp Neurol 296:65–113.

Baizer JS, Ungerleider LG, Desimone R (1991) Organization of visual inputs to the inferior temporal and posterior parietal cortex in macaques. J Neurosci 11:168–190.

Boussaud DR, Desimone R, Ungerleider L (1991) Visual topography of area TEO in the macaque. J Comp Neurol 306:554–575.

Burkhalter A, Felleman DJ, Newsome W, Van Essen DC (1986) Anatomical and physiological asymmetries related to visual areas V3 and VP in macaque extrastriate cortex. Vis Res 26:63–80.

Cusick CG, Kaas JH (1988) Cortical connections of area 18 and dorsolateral visual cortex in squirrel monkey. Vis Neurosci 1:211–237.

Daniel PM, Whitteridge D (1961) The representation of the visual field on the cerebral cortex in monkeys. J Physiol 159:203–221.

Desimone R, Ungerleider, L (1986) Multiple visual areas in the caudal superior temporal sulcus of the macaque. J Comp Neurol 248:164–189.

DeYoe EA, Sisola LC (1991) Distinct pathways link anatomical subdivisions of V4 and V2 and temporal cortex. Soc Neurosci Abstr17:1282.

DeYoe EA, Carman GJ, Bandettini P, Glickman S, Wieser J, Cox R, Miller D, Neitz J (1996) Mapping striate and extrastriate visual areas in human cerebral cortex. Proc Natl Acad Sci USA 93:2382–2386.

Felleman DJ, Van Essen DC (1991) Distributed hierarchical processing in the primate cerebral cortex. Cereb Cortex 1:1–47.

Fenstemaker SB, Albright TD, Gross CG (1986) Organization and neuronal properties of visual area TEO. Soc Neurosci Abstr 11:1012.

Ferrera VP, Nealey TA, Maunsell JH (1991) Magnocellular and parvocellular contributions to macaque area V4. Invest Ophthalmol Vis Sci 32:1117.

Ferrera VP, Nealey, TA, Maunsell, JH (1992) Mixed parvocellular and magnocellular geniculate signals in visual area V4. Nature 358:756–758.

Fleagle JG (1988) Primate adaptation and evolution. San Diego, CA: Academic Press.

Fiorani M, Gattass R, Rosa MGP, Souza, APB (1989) Visual area MT in the *Cebus* monkey: location, visuotopic organization and individual variability. J Comp Neurol 287:98–118.

Gattass R, Gross CG (1981) Visual topography of the striate projection zone (MT) in posterior superior temporal sulcus of the macaque. J Neurophysiol 46:621–638.

Gattass R, Sousa APB, Rosa MGP (1987) Visual topography of V1 in the *Cebus* monkey. J Comp Neurol 259:529–548.

Gattass R, Sousa APB, Gross CG (1988a) Visuotopic organization and extent of V3 and V4 of the macaque. J Neurosci 8:1831–1845.

Gattass R, Sousa APB, Rosa MGP, Piñon MC (1988b) Ventral V3 in the *Cebus* monkey: visual topography and projections to V1. Soc Neurosci Abstr14:202.

Gattass R, Rosa MGP, Sousa APB, Piñon MCGP, Fiorani M (1990) Cortical visual areas of *Cebus apella* monkey. Braz J Med Biol Sci 23:375–393.

Gattass R, Sousa APB, Ungerleider L, Mishkin M (1997) Cortical projections of area V2 in the macaque. Cereb Cortex 7:110–129.

Ghose GM, Ts'o DY (1997) Form processing modules in primate area V4. J Neurophysiol 77:2191–2196.

Hubel DH, Wiesel TN (1974) Uniformity of monkey striate cortex: a parallel relationship between field size, scatter, and magnification factor. J Comp Neurol 158:295–306.

Kaas, JH, Krubitzer LA (1991) The organization of extrastriate visual cortex. In: Neuroanatomy of the visual pathways and their development (Dreher B, Robinson SR, eds), pp. 302–323. London: Macmillan.

Kaas, JH, Morel A (1993) Connections of visual areas of the upper temporal lobe of owl monkeys: the MT crescent and dorsal and ventral subdivisions of FST. J Neurosci 13:534–546.

Le Gros Clark WE (1959) The antecedents of man. Edinburgh: Edinburgh University Press.

Maguire WM, Baizer JS (1984) Visuotopic organization of the prelunate gyrus in rhesus monkey. J Neurosci 4:1690–1704.

Maunsell JHR and Van Essen DC (1987) Topography organization of the middle temporal visual area in the macaque monkey: representational biases and the relationship to callosal connections and myeloarchitectonic boundaries. J Comp Neurol 266:235–255.

Maunsell JHR, Nealey TA, DePriest DD (1990) Magnocellular and parvocellular contributions to responses in the middle temporal visual area (MT) of the macaque monkey. J Neurosci 10:3323–3334.

Morel A, Bullier J (1990) Anatomical segregation of two cortical visual pathways in the macaque monkey. Vis Neurosci 4:555–578.

Nakamura H, Gattass R, Desimone R, Ungerleider LG (1993) The modular organization of projections from areas V1 and V2 to areas V4 and TEO in macaque. J Comp Neurol 13:3681–3691.

Nealey TA, Ferrera VP, Maunsell JH (1991) Magnocellular and parvocellular contributions to the ventral extrastriate cortical processing stream. Soc Neurosci Abstr 17:525.

Neuenschwander S, Gattass R, Sousa APB, Piñon MCGP (1994) Identification and visuotopic organization of areas PO and POd in *Cebus* monkey. J Comp Neurol 340:65–86.

Newsome WT, Maunsell JHR, Van Essen DC (1986) Ventral posterior visual area of the macaque: visual topography and areal boundaries. J Comp Neurol 252:139–153.

Piñon MCGP (1993) Organização Visuotópica da área V4 no macaco *Cebus apella*. PhD thesis, Instituto de Biofísica Carlos Chagas Filho.

Piñon MCGP, Gattass R, Sousa APB (1993) Visuotopic organization of area V4 in *Cebus* monkey. Soc Neurosci Abstr 19:770.

Piñon MCGP, Sousa APB, Gattass R (1990) Topography of cortical efferents of V1 in *Cebus apella* monkey. Soc Neurosci Abstr 16:708.

Roe AW, Ts'o DY (1995) Visual topography in primate V2: multiple representation across functional stripes. J Neurosci 15:3689–3715.

Rosa, MGP (1997) Visuotopic organization of primate extraestriate cortex. In: Cerebral cortex, Vol. 12 (Kaas JH, Rockland KS, Peters A, eds). New York: Plenum Press (in press).

Rosa MGP, Sousa APB, Gattass R (1988) Representation of the visual field in the second visual area in the *Cebus* monkey. J Comp Neurol 275:326–345.

Rosa MGP, Soares JGM, Fiorani M, Gattass R (1993) Cortical afferents of visual area MT in the *Cebus* monkey: possible homologies between New and Old world monkeys. Vis Neurosci 10:827–855.

Schwartz EL (1980) Spatial mapping in the primate sensory projection: analytic structure and relevance to perception. Biol Cybern 25:321–346.

Sereno MI, Allman JM (1990) Cortical visual areas in mammals. In: Neural basis of visual function (Leventhal A, ed.). London: Macmillan.

Sereno MI, McDonald CT, Allman JM (1994) Retinotopic organization of extrastriate cortex in the owl monkey – dorsal and lateral areas. Cereb Cortex 4:601–620.

Sereno MI, Dale AM, Reppas JB, Kwong KK, Belliveau JW, Bradu TJ, Rosen BR, Tootell RBH (1995) Borders of multiple visual areas in humans revealed by functional magnetic resonance imaging. Science 28:889–892.

Sousa APB, Piñon MC, Gattass R, Rosa MGP (1991) Topographical organization of cortical input to striate cortex in the *Cebus* monkey: a fluorescent tracer study. J Comp Neurol 308:665–682.

Stepniewska I, Kaas J (1996) Topographic patterns of V2 cortical connections in macaque monkeys. J Comp Neurol 371:129–152.

Tootell RBH, Dale, AM, Sereno MI, Malach R (1996) New images from human visual cortex. Trends Neurosci 19:481–489.

Ungerleider LG, Mishkin M (1982) Two cortical visual systems. In: Analysis of visual behavior (Ingle DJ, Goodale MA, Mansfield RJ, eds). Cambridge, MA: MIT Press.

Van Essen DC, Gallant JL (1994) Neural mechanisms of form and motion processing in the primate visual system. Neuron 13:1–10.

Van Essen DC, Zeki SM (1978) The topographic organization of rhesus monkey prestriate cortex. J Physiol 277:193–226.

Van Essen DC, Newsome WT, Maunsell, JHR (1984) The visual field representation in striate cortex of the macaque monkey: asymmetries, anisotropies and individual variability. Vis Res 24:429–448.

Van Essen DC, Felleman DJ, DeYoe EA, Olavarria J, Knierim J (1990) Modular and hierarchical organization of extrastriate visual cortex in the macaque monkey. Cold Spring Harbor Symposia 55:679–696.

Van Essen DC, Anderson CH, Felleman DJ (1992) Information processing in the primate visual system: an integrated systems perspective. Science 255:419–423.

Weller RE, Kaas JH (1985) Cortical projections of the dorso-lateral visual

area in owl monkeys: the prestriate relay to inferior temporal cortex. J Comp Neurol 211:193–214.

Youakim M, Baizer JS (1990) Distribution of response properties across topographic subdivisions of macaque prelunate gyrus. Soc Neurosci Abstr 16:1220.

Zeki SM (1971) Convergent input from striate cortex (area 17) to the cortex of the superior temporal sulcus in the rhesus monkey. Brain Res 28:338–340.

Zeki SM (1978) Uniformity and diversity of structure and function in rhesus monkey prestriate visual cortex. J Physiol 277:273–290.

Zeki SM (1993) A vision of the brain. Oxford: Blackwell Science.

Zeki SM (1996) Are areas TEO and PIT of monkey visual cortex wholly distinct from the fourth visual complex (V4 complex)? Proc R Soc Lond B 263:1539–1544.

Zeki SM, Shipp S (1989) Modular connections between areas V2 and V4 of macaque monkey visual cortex. Eur J Neurosci 1:494–506.